

See discussions, stats, and author profiles for this publication at: <https://www.researchgate.net/publication/257645956>

Multicomponent Reactions for de Novo Synthesis of BODIPY Probes: In Vivo Imaging of Phagocytic Macrophages

ARTICLE in JOURNAL OF THE AMERICAN CHEMICAL SOCIETY · OCTOBER 2013

Impact Factor: 12.11 · DOI: 10.1021/ja408093p · Source: PubMed

CITATIONS

21

READS

54

8 AUTHORS, INCLUDING:



[Sara Preciado](#)

Enantia, S.L., Barcelona, Spain

16 PUBLICATIONS 137 CITATIONS

SEE PROFILE



[Richard J Mellanby](#)

The University of Edinburgh

120 PUBLICATIONS 1,118 CITATIONS

SEE PROFILE



[Rodolfo Lavilla](#)

107 PUBLICATIONS 1,768 CITATIONS

SEE PROFILE



[Marc Vendrell](#)

The University of Edinburgh

38 PUBLICATIONS 1,143 CITATIONS

SEE PROFILE

Multicomponent Reactions for *de Novo* Synthesis of BODIPY Probes: *In Vivo* Imaging of Phagocytic Macrophages

Ana Vázquez-Romero,^{†,⊥} Nicola Kielland,^{†,⊥} María J. Arévalo,[‡] Sara Preciado,[†] Richard J. Mellanby,[§] Yi Feng,[§] Rodolfo Lavilla,^{*,†,||} and Marc Vendrell^{*,§}

[†]Barcelona Science Park, Baldiri Reixac 10-12, 08028 Barcelona, Spain

[‡]Escuela Politécnica, Universidad Extremadura, Avda. de la Universidad s/n, 10003 Cáceres, Spain

[§]MRC Centre for Inflammation Research, Queen's Medical Research Institute, University of Edinburgh, Edinburgh EH16 4TJ, United Kingdom

^{||}Laboratory of Organic Chemistry, Faculty of Pharmacy, University of Barcelona, Avda. Joan XXIII s/n, 08028 Barcelona, Spain

S Supporting Information

ABSTRACT: Multicomponent reactions are excellent tools to generate complex structures with broad chemical diversity and fluorescent properties. Herein we describe the adaptation of the fluorescent BODIPY scaffold to multicomponent reaction chemistry with the synthesis of BODIPY adducts with high fluorescence quantum yields and good cell permeability. From this library we identified one BODIPY derivative (PhagoGreen) as a low-pH sensing fluorescent probe that enabled imaging of phagosomal acidification in activated macrophages. The fluorescence emission of PhagoGreen was proportional to the degree of activation of macrophages and could be specifically blocked by bafilomycin A, an inhibitor of phagosomal acidification. PhagoGreen does not impair the normal functions of macrophages and can be used to image phagocytic macrophages *in vivo*.

Fluorescent probes are chemical entities of enormous importance in biomedical research and medical imaging. In the context of fluorescence live cell imaging, they enable real-time tracking of biomolecules, metabolites and cells under physiological conditions without altering regular cellular functions.¹ The 4,4-difluoro-4-bora-3a,4a-diaza-s-indacene (BODIPY) scaffold has played a pivotal role in fluorescent probe development, and it is one of the most exploited fluorophores due to its excellent photophysical properties.² Amine and carboxylic acid-derivatized BODIPY dyes are readily available, and have been conjugated to numerous biomolecules to develop fluorescent compounds to enable biological interrogation. This approach has rendered a wide variety of BODIPY-based cell imaging probes.³ Combinatorial strategies have recently expanded the chemical diversity of the BODIPY core. These strategies employ efficient and stepwise reactions (e.g., Knoevenagel condensation, 'click' chemistry) to implement structural diversification into a presynthesized BODIPY scaffold.⁴ Subsequent high-throughput screenings of the resulting libraries have significantly accelerated the discovery of new fluorescent probes.⁵ We envisioned that the use of multicomponent reactions (MCRs)⁶ for the synthesis of BODIPY fluorescent probes would lead to novel complex

structures that are difficult to prepare by conventional synthetic strategies. MCRs can increase the chemical diversity of BODIPY dyes with the formation of unusual C–C bonds and give BODIPY compounds with unexplored chemical connectivity and potentially new features as imaging probes.

Our group and others have described MCRs to prepare complex fluorescent molecules based on 2,6-cyanodianilines,⁷ isoquinolines,⁸ naphthalimides,⁹ benzoazepines¹⁰ and imidazoles.¹¹ Balakirev and co-workers recently reported the combinatorial exploitation of three component Ugi MCRs in droplet arrays to successfully discover new fluorophores with drug-like properties.¹² Whereas these examples proved the suitability of MCRs to generate *de novo* fluorescent structures, they employed scaffolds with inherent limitations as fluorophores (e.g., short emission wavelengths, low extinction coefficients, poor quantum yields, compromised cell permeability).

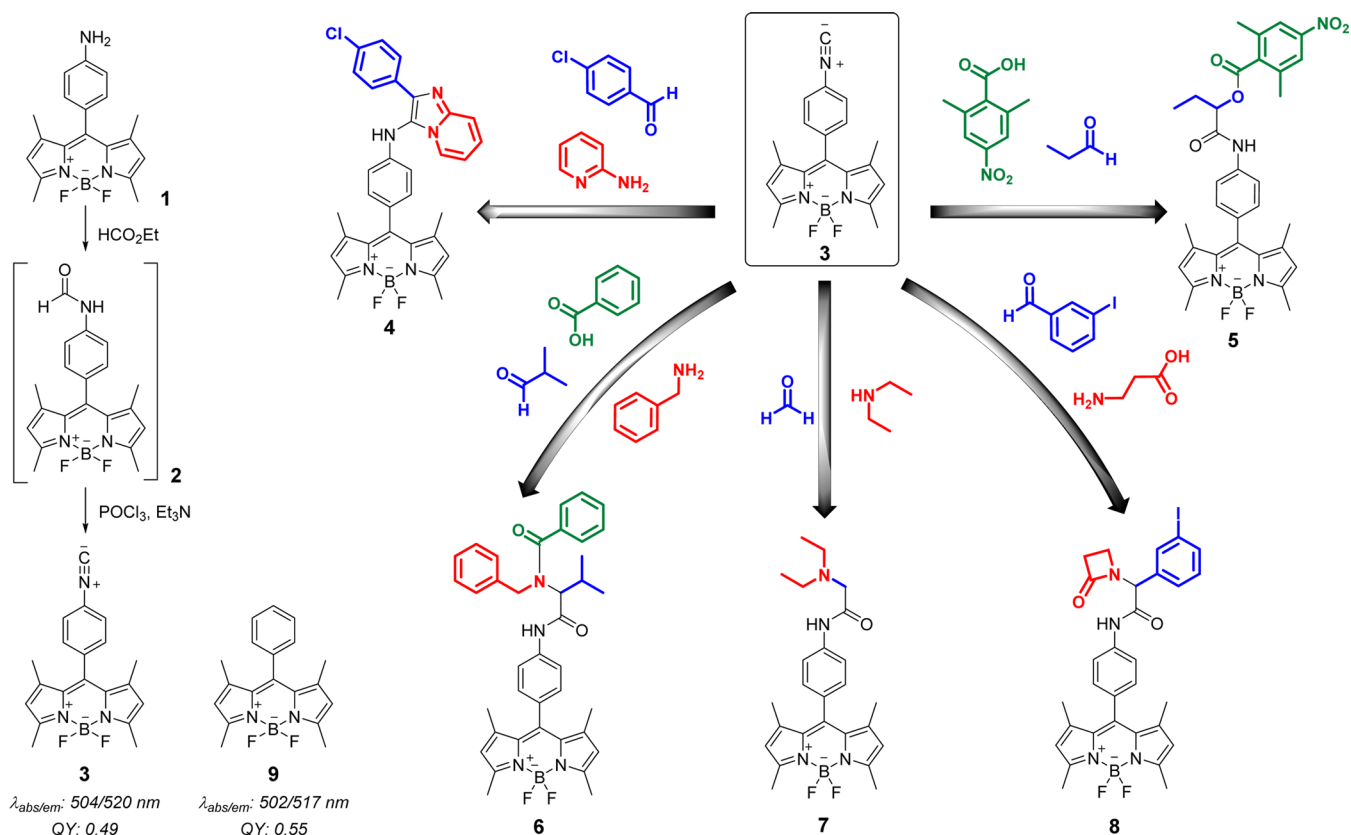
The adaptation of MCRs to the highly fluorescent and cell permeable BODIPY scaffold provides a practical platform to develop novel compounds with unexpected features as cell imaging fluorescent probes. Since the most versatile MCRs are based on isonitrile chemistry,¹³ we prepared an isonitrile-BODIPY scaffold (**3**) compatible with several MCRs (Scheme 1). Compound **3** was prepared in a two-step reaction from the BODIPY aniline **1**, obtained by reduction of the corresponding nitro compound.¹⁴ The BODIPY aniline **1** was formylated with HCO₂Et to render the formamide **2**, which was subsequently dehydrated under standard conditions with POCl₃ to afford the isonitrile **3**. Notably, the isonitrile functional group did not affect the fluorescent properties of the BODIPY core (**9**) (Figure S1 and Table S1 in Supporting Information (SI)). To the best of our knowledge, this is the first report of an isonitrile-functionalized BODIPY dye and its subsequent derivatization using MCRs.

We employed **3** as the starting material for a number of isonitrile-based MCRs, namely Passerini,¹⁵ Bienaymé–Blackburn–Groebcke,¹⁶ and three variants of the Ugi-MCR¹⁷ (Scheme 1). We performed a Bienaymé–Blackburn–Groebcke MCR with **3**, α -aminopyridine, and 4-chlorobenzaldehyde to

Received: August 5, 2013

Published: October 10, 2013

Scheme 1. Synthesis of an Isonitrile-BODIPY Scaffold and Its Derivatization Using Different MCRs



obtain the azaindole 4. A conventional Passerini reaction of 3 with propanal and 2,6-dimethyl-4-nitrobenzoic acid rendered the adduct 5. A four-component Ugi MCR with isobutylaldehyde, benzylamine, and benzoic acid afforded compound 6, whereas the β -amino acid variation led to the β -lactam 8. The adduct 7 was obtained with a variant of the Ugi MCR using formaldehyde and diethylamine. Notably, all adducts (4–8) were isolated in good yields (see details and characterization data in SI) and retained the characteristic fluorescent properties of the BODIPY core (Figure S1 and Table S1 in SI). The synthesis of this collection of BODIPY adducts confirms that the reactivity of the isonitrile group in different MCRs is not hampered by the BODIPY structure. Altogether, the results validate isonitrile-based MCRs as a synthetic platform for the diversification of the BODIPY scaffold toward fluorescent conjugates that might be difficult to prepare by conventional strategies.

We assessed the cell permeability of compounds 3–8 by imaging their localization in live A549 cells together with different intracellular trackers (Figures S2 and S3 in SI) and observed that all adducts readily entered cells at concentrations in the nanomolar range. While most adducts stained the cytoplasm and some lysosomes, compound 7 exhibited a distinctive, vesicle-like staining pattern (Figure 1). We examined the subcellular localization of 7 in different cell lines by colocalization with LysoTracker Red, a fluorescent dye that labels acidic organelles (Figures S4 and S5 in SI).

The similar staining patterns of 7 and LysoTracker Red indicated that 7 is an acidotropic fluorescent molecule with bright fluorescence emission in subcellular acidic environments. Compound 7 has a pK_a of 5.76 ± 0.07 (Figure S6 in SI) and

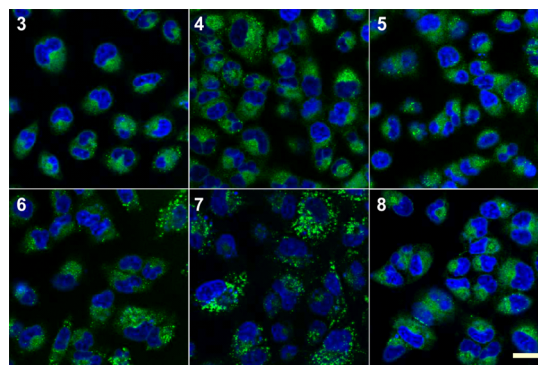


Figure 1. Cell permeability of BODIPY adducts in live cell imaging. A549 cells were incubated with compounds 3–8 (250 nM) for 30 min and imaged under the confocal fluorescence microscope. DAPI was used for nuclear counterstaining. Scale bar: 20 μm .

higher sensitivity to pH than LysoTracker Red (Figure S7 in SI).

We envisaged that these remarkable properties of 7 as a cell permeable fluorescent probe for acidic microenvironments may be applied to imaging phagosomal acidification in macrophages. Macrophages are immune cells with key roles in inflammation and tissue homeostasis. Macrophages ingest pathogens and particles by phagocytosis. During the course of phagocytosis the maturation and fusion of endosomes leads to a progressive phagosomal acidification.¹⁸ Most currently used probes for activated macrophages target the recognition of enzymes (e.g., cathepsins) or cell surface receptors (e.g., folate, integrins).¹⁹ Bogoy and co-workers recently described fluorescent probes to

monitor legumain activity in the acidic organelles of activated macrophages.²⁰

We acquired fluorescent images of RAW264.7 macrophages treated with compound 7 before and after activation with zymosan (Figure 2). Zymosan is a glucan from the yeast cell

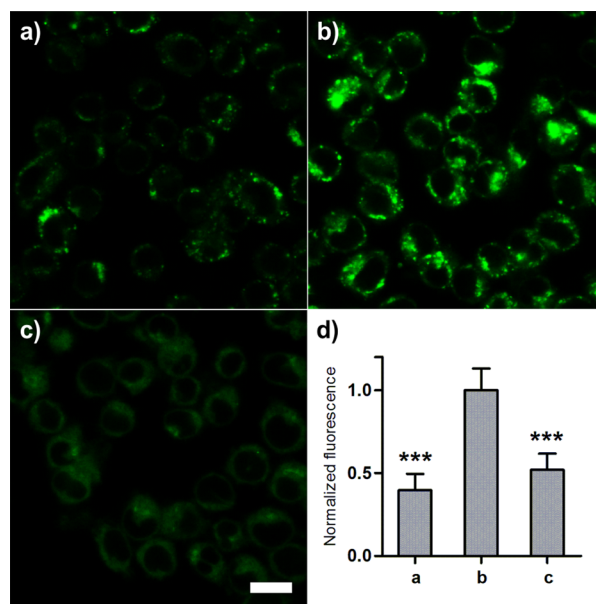


Figure 2. Compound 7 stains macrophages undergoing phagosomal acidification. RAW264.7 cells (preincubated or not with zymosan) were treated with 7 (100 nM) for 15 min and imaged by confocal microscopy. Fluorescence staining of 7 in (a) nonactivated macrophages, (b) zymosan-activated macrophages, and (c) zymosan-activated macrophages treated with bafilomycin A (100 nM); (d) quantification of fluorescence emission represented as means ($n = 4$) and error bars as SD, *** for $p < 0.005$ compared to b. Scale bar: 20 μm .

wall that induces phagosomal acidification in macrophages.²¹ Zymosan-activated macrophages displayed bright fluorescence in the perinuclear region, where most phagosomes are located (Figure 2b). The fluorescence intensity was significantly brighter in zymosan-activated than in nonactivated macrophages (Figure 2d). The staining of 7 was proportional to the extent of the zymosan treatment, proving that, unlike Lysotracker Red, the emission of 7 correlates with the degree of activation of macrophages (Figures S8 and S9 in SI). We confirmed that the staining of 7 relies on the acidification of the phagosomes. As shown in Figure 2c, the staining of zymosan-activated macrophages decreased upon treatment with bafilomycin A, an inhibitor of the vacuolar ATPase that is required for phagosomal acidification.²²

We observed that compound 7 was nontoxic to macrophages at 500 nM, even at long incubation times (Figure S10 in SI). We also studied whether the treatment with compound 7 affected the secretion of $\text{TNF-}\alpha$ and IL-6, two major cytokines released by macrophages. As shown in Figure 3, there were no significant differences in the levels of $\text{TNF-}\alpha$ and IL-6 secreted by nontreated and 7-treated macrophages before or after stimulation with liposaccharide S (LPS). These results validate 7 as a fluorescent probe to image phagocytic macrophages without impairing their normal function. On account of these observations, compound 7 was named as PhagoGreen.

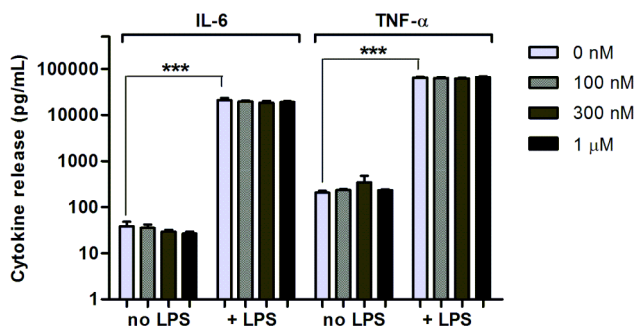


Figure 3. Cytokine release by macrophages after incubation with PhagoGreen. RAW264.7 cells (with or without PhagoGreen) were stimulated with LPS (100 ng/mL) for 18 h. The levels of $\text{TNF-}\alpha$ and IL-6 in the supernatants were measured by ELISA. Values represented as means ($n = 4$) and error bars as SD, *** for $p < 0.0001$.

Finally, we examined the application of PhagoGreen to image phagocytic macrophages *in vivo*. Zebrafish embryos expressing mCherry-labeled phagocytic macrophages²³ were imaged after incubation with PhagoGreen (Figure 4).

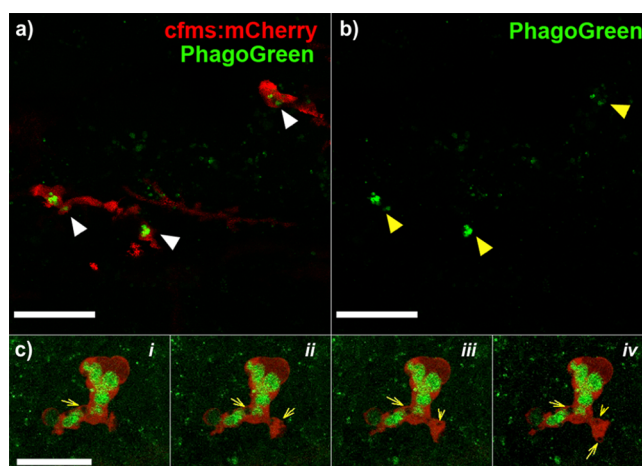


Figure 4. PhagoGreen enables *in vivo* imaging of phagocytic macrophages. Transgenic zebrafish with mCherry-labeled macrophages were treated with PhagoGreen (600 nM) for 30 min and imaged by confocal microscopy. (a) Images from a time-lapse movie (Video S1) showing the phagosomal localization of PhagoGreen (white arrowheads) demonstrated by the surrounding red fluorescence of cytoplasmic mCherry; (b) single channel image of (a) showing brighter fluorescence in mature phagosomes (yellow arrowheads); (c) i–iv: sequential images from a time-lapse movie (Video S2) of an actively engulfing macrophage, where the mature phagosome is brightly green fluorescent while the newly formed phagosome is devoid of green fluorescence (yellow arrows). Scale bars (a,b): 20 μm , (c): 15 μm .

As shown in Figure 4, PhagoGreen stained phagosomes in mCherry-labeled phagocytic macrophages. Time-lapse imaging confirmed that PhagoGreen-stained macrophages were actively phagocytic (Video S1). Furthermore, high-resolution time-lapse imaging showed that PhagoGreen did not stain early phagosomes (Figure 4c; Video S2), which corroborates our observation that the mechanism of staining for PhagoGreen relies on phagosomal acidification.

In conclusion, we described the first adaptation of multi-component reaction chemistry to prepare BODIPY-based imaging probes with broad and unexplored chemical diversity.

A novel isonitrile-BODIPY scaffold was successfully used in different MCRs to render highly fluorescent and cell permeable BODIPY adducts. From our library we identified PhagoGreen as a pH-sensitive fluorescent probe to image phagosomal acidification in macrophages. We corroborated the staining mechanism of PhagoGreen in macrophages by different treatments with zymosan, and its specific blocking with bafilomycin A, an inhibitor of phagosomal acidification. PhagoGreen will facilitate the study of the mechanisms underlying macrophage-mediated phagocytosis, as it can image phagocytic macrophages *in vivo* and in real time without impairing the normal physiology of macrophages.

■ ASSOCIATED CONTENT

■ Supporting Information

Synthetic procedures, full characterization and spectral data for compounds 1–9, cell viability assays, imaging data including videos. This material is available free of charge via the Internet at <http://pubs.acs.org>.

■ AUTHOR INFORMATION

Corresponding Authors

rlavilla@pcb.ub.es
mwendrel@staffmail.ed.ac.uk

Author Contributions

[†]These authors contributed equally.

Notes

The authors declare no competing financial interest.

■ ACKNOWLEDGMENTS

This work was supported by DGICYT–Spain (BQU-CTQ2012-30930) and Generalitat de Catalunya (2009SGR 1024). Grupo Ferrer (Barcelona, Spain) is thanked for financial support. M.V. acknowledges the support of the Medical Research Council and the FP7Marie Curie Career Integration Grant. Y.F. is supported by a Wellcome Trust Sir Henry Dale Fellowship (100104/Z/12/Z), and R.J.M. is funded by a Wellcome Trust Intermediate Clinical Fellowship.

■ REFERENCES

- (1) (a) Kobayashi, H.; Ogawa, M.; Alford, R.; Choyke, P. L.; Urano, Y. *Chem. Rev.* **2010**, *110*, 2620. (b) Chan, J.; Dodani, S. C.; Chang, C. J. *Nat. Chem.* **2012**, *4*, 973. (c) Vendrell, M.; Zhai, D.; Er, J. C.; Chang, Y. T. *Chem. Rev.* **2012**, *112*, 4391. (d) Yuan, L.; Lin, W.; Zheng, K.; He, L.; Huang, W. *Chem. Soc. Rev.* **2013**, *42*, 622. (e) Wysocki, L. M.; Lavis, L. D. *Curr. Opin. Chem. Biol.* **2011**, *15*, 752.
- (2) (a) Loudet, A.; Burgess, K. *Chem. Rev.* **2007**, *107*, 4891. (b) Ulrich, G.; Ziessel, R.; Harriman, A. *Angew. Chem., Int. Ed.* **2008**, *47*, 1184. (c) Boens, N.; Leen, V.; Dehaen, W. *Chem. Soc. Rev.* **2012**, *41*, 1130.
- (3) (a) Myochin, T.; Hanaoka, K.; Komatsu, T.; Terai, T.; Nagano, T. *J. Am. Chem. Soc.* **2012**, *134*, 13730. (b) Michel, B. W.; Lippert, A. R.; Chang, C. J. *J. Am. Chem. Soc.* **2012**, *134*, 15668. (c) Dodani, S. C.; Leary, S. C.; Cobine, P. A.; Winge, D. R.; Chang, C. J. *J. Am. Chem. Soc.* **2011**, *133*, 8606. (d) Isik, M.; Ozdemir, T.; Turan, I. S.; Kolemene, S.; Akkaya, E. U. *Org. Lett.* **2013**, *15*, 216. (e) Gavande, N.; Kim, H.-L.; Doddareddy, M. R.; Johnston, G. A. R.; Chebib, M.; Hanrahan, J. R. *ACS Med. Chem. Lett.* **2013**, *4*, 402. (f) Komatsu, T.; Urano, Y.; Fujikawa, Y.; Kobayashi, T.; Kojima, H.; Terai, T.; Hanaoka, K.; Nagano, T. *Chem. Commun.* **2009**, 7015.
- (4) (a) Lee, J. S.; Kang, N. Y.; Kim, Y. K.; Samanta, A.; Feng, S.; Kim, H. K.; Vendrell, M.; Park, J. H.; Chang, Y. T. *J. Am. Chem. Soc.* **2009**, *131*, 10077. (b) Vendrell, M.; Krishna, G. G.; Ghosh, K. K.; Zhai, D.; Lee, J. S.; Zhu, Q.; Yau, Y. H.; Shochat, S. G.; Kim, H.; Chung, J.; Chang, Y. T. *Chem. Commun.* **2011**, *47*, 8424. (c) Zhai, D.; Lee, S. C.; Vendrell, M.; Leong, L. P.; Chang, Y. T. *ACS Comb. Sci.* **2012**, *14*, 81.
- (d) Er, J. C.; Tang, M. K.; Chia, C. G.; Liew, H.; Vendrell, M.; Chang, Y. T. *Chem. Sci.* **2013**, *4*, 2168.
- (5) (a) Ahn, Y. H.; Lee, J. S.; Chang, Y. T. *J. Am. Chem. Soc.* **2007**, *129*, 4510. (b) Lee, J. S.; Kim, H. K.; Feng, S.; Vendrell, M.; Chang, Y. T. *Chem. Commun.* **2011**, *47*, 2339.
- (6) (a) For an overview, see: *Multicomponent reactions*; Zhu, J.; Bienaymé, H., Eds.; Wiley-VCH: Weinheim, 2005. (b) Domling, A.; Wang, W.; Wang, K. *Chem. Rev.* **2012**, *112*, 3083.
- (7) Cui, S. L.; Lin, X. F.; Wang, Y. G. *J. Org. Chem.* **2005**, *70*, 2866.
- (8) Kielland, N.; Vendrell, M.; Lavilla, R.; Chang, Y. T. *Chem. Commun.* **2012**, *48*, 7401.
- (9) Rotstein, B. H.; Mourtada, R.; Kelley, S. O.; Yudin, A. K. *Chem.—Eur. J.* **2011**, *17*, 12257.
- (10) Pan, H. R.; Wang, X. R.; Yan, C. X.; Sun, Z. X.; Cheng, Y. Org. *Biomol. Chem.* **2011**, *9*, 2166.
- (11) (a) Bienaymé, H.; Bouzid, K. *Angew. Chem., Int. Ed.* **1998**, *37*, 2234. (b) Wang, W.; Cao, H.; Wolf, S.; Camacho-Horvitz, M. S.; Holak, T. A.; Domling, A. *Bioorg. Med. Chem.* **2013**, *21*, 3982.
- (12) Burchak, O. N.; Mughlerli, L.; Ostuni, M.; Lacapere, J. J.; Balakirev, M. Y. *J. Am. Chem. Soc.* **2011**, *133*, 10058.
- (13) (a) For an overview, see: *Isoyanide Chemistry*; Nenadjenko, V. G., Ed.; Wiley-VCH: Weinheim, 2012. (b) Domling, A. *Chem. Rev.* **2006**, *106*, 17. (c) Domling, A.; Ugi, I. I. *Angew. Chem., Int. Ed.* **2000**, *39*, 3168.
- (14) Imahori, H.; Norieda, H.; Yamada, H.; Nishimura, Y.; Yamazaki, I.; Sakata, Y.; Fukuzumi, S. *J. Am. Chem. Soc.* **2001**, *123*, 100.
- (15) Banfi, L.; Riva, R. *Org. React.* **2005**, *65*, 1.
- (16) (a) Bienaymé, H.; Bouzid, K. *Angew. Chem., Int. Ed.* **1998**, *37*, 2234. (b) Blackburn, C.; Guan, B.; Fleming, P.; Shiosaki, K.; Tsai, S. *Tetrahedron Lett.* **1998**, *39*, 3635. (c) Groebcke, K.; Weber, L.; Mehlin, F. *Synlett* **1998**, 661.
- (17) Ugi, I.; Steinbruckner, C. *Angew. Chem.* **1960**, *72*, 267.
- (18) Jiang, L.; Salao, K.; Li, H.; Rybicka, J. M.; Yates, R. M.; Luo, X. W.; Shi, X. X.; Kuffner, T.; Tsai, V. W. W.; Husaini, Y.; Wu, L.; Brown, D. A.; Grewal, T.; Brown, L. J.; Curmi, P. M. G.; Breit, S. N. *J. Cell Sci.* **2012**, *125*, 5479.
- (19) (a) Verdoes, M.; Edgington, L. E.; Scheeren, F. A.; Leyva, M.; Blum, G.; Weiskopf, K.; Bachmann, M. H.; Ellman, J. A.; Bogoy, M. *Chem. Biol.* **2012**, *19*, 619. (b) Chen, W. T.; Khazaie, K.; Zhang, G.; Weissleder, R.; Tung, C. H. *Mol. Imaging* **2005**, *4*, 67. (c) Waldeck, J.; Hager, F.; Holtke, C.; Lanckohr, C.; von Wallbrunn, A.; Torsello, G.; Heindel, W.; Theilmeier, G.; Schafers, M.; Bremer, C. *J. Nucl. Med.* **2008**, *49*, 1845. (d) Saxena, A.; Kessinger, C. W.; Thompson, B.; McCarthy, J. R.; Iwamoto, Y.; Lin, C. P.; Jaffer, F. A. *Mol. Imaging Biol.* **2013**, *15*, 282.
- (20) (a) Lee, J.; Bogoy, M. *ACS Chem. Biol.* **2010**, *5*, 233. (b) Edgington, L. E.; Verdoes, M.; Ortega, A.; Withana, N. P.; Lee, J.; Syed, S.; Bachmann, M. H.; Blum, G.; Bogoy, M. *J. Am. Chem. Soc.* **2013**, *135*, 174.
- (21) Haggie, P. M.; Verkman, A. S. *J. Biol. Chem.* **2007**, *282*, 31422.
- (22) Lukacs, G. L.; Rotstein, O. D.; Grinstein, S. *J. Biol. Chem.* **1990**, *265*, 21099.
- (23) Gray, C.; Loynes, C. A.; Whyte, M. K.; Crossman, D. C.; Renshaw, S. A.; Chico, T. J. *Thromb. Haemost.* **2011**, *105*, 811.